Human Molecular Genetics, 2008, Vol. 17, No. 19 **2956–2966**
doi:10.1093/hmg/ddn194
Advance Access published on July 9, 2008

Neurofibromin regulates somatic growth through the hypothalamic–pituitary axis

Balazs Hegedus[1], Tu-Hsueh Yeh[1,2], Da Yong Lee[1], Ryan J. Emnett[1], Jia Li[1] and David H. Gutmann[1,*]

[1]Department of Neurology, Washington University School of Medicine, St Louis, MO 63110, USA and
[2]Department of Neurology, Chang Gung Memorial Hospital and University, Taipei, Taiwan, Republic of China

Received March 17, 2008; Revised May 21, 2008; Accepted July 3, 2008

To study the role of the neurofibromatosis-1 (NF1) gene in mammalian brain development, we recently generated mice in which *Nf1* gene inactivation occurs in neuroglial progenitor cells using the brain lipid binding protein (BLBP) promoter. We found that *Nf1*^{BLBP}CKO mice exhibit significantly reduced body weights and anterior pituitary gland sizes. We further demonstrate that the small anterior pituitary size reflects loss of neurofibromin expression in the hypothalamus, leading to reduced growth hormone releasing hormone, pituitary growth hormone (GH) and liver insulin-like growth factor-1 (IGF1) production. Since neurofibromin both negatively regulates Ras activity and positively modulates cAMP levels, we examined the signaling pathway responsible for these abnormalities. While BLBP-mediated expression of an activated Ras molecule did not recapitulate the body weight and hypothalamic/pituitary defects, treatment of *Nf1*^{BLBP}CKO mice with rolipram to increase cAMP levels resulted in a partial restoration of the body weight phenotype. Furthermore, conditional expression of the Ras regulatory GAP domain of neurofibromin also did not rescue the body weight or *Igf1* mRNA defects in *Nf1*^{BLBP}CKO mice. Collectively, these data demonstrate a critical role for neurofibromin in hypothalamic–pituitary axis function and provide further insights into the short stature and GH deficits seen in children with NF1.

INTRODUCTION

Short stature is a common problem in children and young adults with the inherited tumor predisposition, neurofibromatosis type 1 (NF1). Thirteen to eighteen percent of individuals with NF1 exhibit stature measurements greater than two standard deviations below the population norm (1,2). While multiple etiologies could underlie this growth defect, abnormal hypothalamic–pituitary axis function has been hypothesized to play a causative role (3). In the largest study of pituitary function in children with NF1 and short stature, nearly 80% of these children (15/19 patients) were found to have growth hormone (GH) deficiency in the absence of suprasellar abnormalities on neuroimaging (4).

The *NF1* gene encodes a large cytoplasmic protein, termed neurofibromin, which was originally demonstrated to function as a negative regulator of Ras (5). Within the neurofibromin predicted coding sequence are ~300 amino acids which comprise the GTPase-activating protein (GAP) domain (6–8). Consistent with the proposed role of neurofibromin as a Ras GAP, loss of *Nf1* expression in numerous mammalian cell types results in increased Ras activity and downstream MAPK/Akt signaling (9,10). In addition, replacement of this GAP-related domain in astrocytes, fibroblasts and Schwann cells restores normal Ras activity and reverses the growth advantage that results from *Nf1* inactivation (11–13).

While neurofibromin is thought to primarily regulate cell growth by modulating Ras activity, studies in both *Drosophila* and mouse tissues have shown that neurofibromin also positively regulates intracellular cAMP levels (14–16). Analysis of *Nf1*−/− embryonic forebrain homogenates and primary neuronal cultures demonstrated lower cAMP levels compared with wild-type (WT) controls (16). In astrocytes, neurofibromin regulation of cAMP contributes to the increased cell survival and growth observed in cultured *Nf1*−/− astrocytes (14,17). During differentiation from neural progenitor cells, neurofibromin regulates neuronal maturation *in vitro* and *in vivo* in a cAMP-dependent manner (18). In contrast, the

*To whom correspondence should be addressed at: Department of Neurology, Washington University School of Medicine, PO Box 8111, 660 South Euclid Avenue, St Louis, MO 63110, USA. Email: gutmannd@neuro.wustl.edu

increased gliogenesis that results from neurofibromin deficiency in neuroglial progenitor cells requires Ras and Akt activation *in vivo* (18). These studies suggest that neurofibromin may function in the mammalian central nervous system (CNS) by modulating either Ras- or cAMP-dependent pathways.

Relevant to the short stature observed in individuals with NF1, previous studies in *Drosophila* have shown that *Nf1* mutant flies have reduced body size at the larval, pupal and adult stages, which was not restored by manipulating Ras1 signaling (19). Instead, the size defect was partially corrected by the expression of an activated adenosine 3′, 5′-monophosphate-dependent protein kinase (PKA) molecule. Subsequent studies from this group revealed that this mutant *Drosophila* phenotype reflects de-regulated Ras2 function in neurofibromin-deficient fly tissues (20). However, in *Nf1*−/− mouse cells, R-Ras2 activation leads to increased signaling through the phosphatidylinositol 3-kinase (PI3-kinase) and MAP kinase pathways (21). To explore the role of the *NF1* gene in body size regulation in mice, we used a recently developed mouse strain in which *Nf1* inactivation occurs in neural stem/progenitor cells (*Nf1*^{BLBP}CKO mice). In this report, we demonstrate that neurofibromin regulates hypothalamic–pituitary axis function in a Ras-independent fashion.

RESULTS

Nf1^{BLBP}CKO mice exhibit reduced anterior pituitary gland size

We inactivated the *Nf1* gene in embryonic neural stem/progenitor cells within the developing CNS by Cre-mediated recombination using a 1.6 kb fragment of the mouse *Blbp* promoter as previously reported (18). Cre recombinase activity was detected throughout the mouse CNS using either BLBP-Cre;Rosa-YFP or BLBP-Cre;LSL-myr-Akt reporter mouse crosses (18,22). *Nf1*^{BLBP}CKO mice were born at the expected Mendelian ratios and initially appeared normal. However, during the first week of life, *Nf1*^{BLBP}CKO mice displayed severe growth retardation, resulting in >60% lower body weights compared with BLBP-Cre; *Nf1*$^{flox/wt}$ (HET) or WT littermates by 3 weeks of age (Fig. 1A and B). No normalization of body weight was observed later during postnatal development: The few mice that survived to 2 or 3 months of age retained this growth deficit, reaching about 30% of the weight of WT littermates (data not shown). Both male and female mice exhibited similar growth retardation. Complete necropsies of *Nf1*^{BLBP}CKO mice failed to reveal any gross or microscopic abnormalities to account for the observed growth failure, and abundant milk was detected in the stomachs of *Nf1*^{BLBP}CKO pups (data not shown). Upon careful examination of the skull base after removal of the brain, the pituitary gland was found to be smaller in *Nf1*^{BLBP}CKO mice (Fig. 1C). Following dissection of the pituitary gland, the posterior lobes were of normal size in mice of all genotypes (Fig. 1D); however, the anterior pituitary was significantly smaller in *Nf1*^{BLBP}CKO mice compared with heterozygous or WT littermates (Fig. 1E).

Impaired hypothalamic releasing hormone production in *Nf1*^{BLBP}CKO mice

Early *Nf1* gene inactivation in embryonic neural stem/progenitor cells leads to widespread loss of neurofibromin expression throughout the CNS, including the hypothalamus. Immunohistochemical staining demonstrated a 75% reduction in the number of neurofibromin-expressing cells (Fig. 2A) and a 60% reduction in *Nf1* mRNA by quantitative real-time PCR (qPCR) in the postnatal hypothalamus (Fig. 2B). In contrast, there was no significant change in *Nf1* mRNA expression in the pituitary gland.

Since growth hormone releasing hormone (GHRH) is a critical factor in the development of the hypothalamic–pituitary axis (23), we analyzed GHRH expression by immunohistochemistry. We found a significant reduction in GHRH staining within the median eminence, the primary capillary network of the hypophyseal portal system (Fig. 2C). Next, we sought to determine whether the production of releasing hormones in neuroendocrine cells of the hypothalamus was altered in *Nf1*^{BLBP}CKO mice. Using qPCR, we found a 40–60% reduction in the levels of *Ghrh*, *Gnrh* and *Trh* mRNA in *Nf1*^{BLBP}CKO mice compared with WT controls (Fig. 2D). Interestingly, the pattern of growth retardation described in transgenic rat and mice models with reduced GHRH production or impaired GHRH receptor function was similar to the phenotype we observed in *Nf1*^{BLBP}CKO mice (24–26). These observations coupled with our results suggest that neurofibromin is an important regulator of the hypothalamic–pituitary axis and *Ghrh* expression.

Nf1^{BLBP}CKO mice have altered hormone production in the pituitary gland

As GHRH is a major regulator of postnatal pituitary development, we quantified the number of proliferating cells in the pituitary gland (Fig. 3A). There was a 3-fold reduction in the number of BrdU-incorporating cells throughout the anterior lobe of pituitary glands from *Nf1*^{BLBP}CKO mice compared with WT or HET littermate controls at postnatal day (PN) 18 (Fig. 3B). No changes in BrdU incorporation were seen in the neurohypophysis (data not shown). In addition, we found that the number of apoptotic cells was unchanged in either part of the gland, as determined by TUNEL labeling (data not shown). To determine whether neurofibromin loss in the hypothalamus resulted in impaired pituitary hormone production, we next counted the number of ACTH-expressing cells in the anterior lobe by immunohistochemistry (Fig. 3C). The number of ACTH-labeled cells in the gland was not decreased in *Nf1*^{BLBP}CKO mice compared with littermate controls (Fig. 3D). Moreover, there was no change in the levels of *Tsh1β* mRNA in *Nf1*^{BLBP}CKO mouse pituitary glands at PN18 by qPCR (Fig. 3E).

In contrast, GH and prolactin (PRL) mRNA levels were significantly reduced in the pituitary glands of *Nf1*^{BLBP}CKO mice (Fig. 3E). To determine the functional consequence of reduced GH production in *Nf1*^{BLBP}CKO mice, we measured *Igf1* mRNA levels in the liver at PN18 as a surrogate marker of circulating GH. We found a 65% reduction in liver *Igf1* mRNA levels in *Nf1*^{BLBP}CKO mice compared with littermate controls

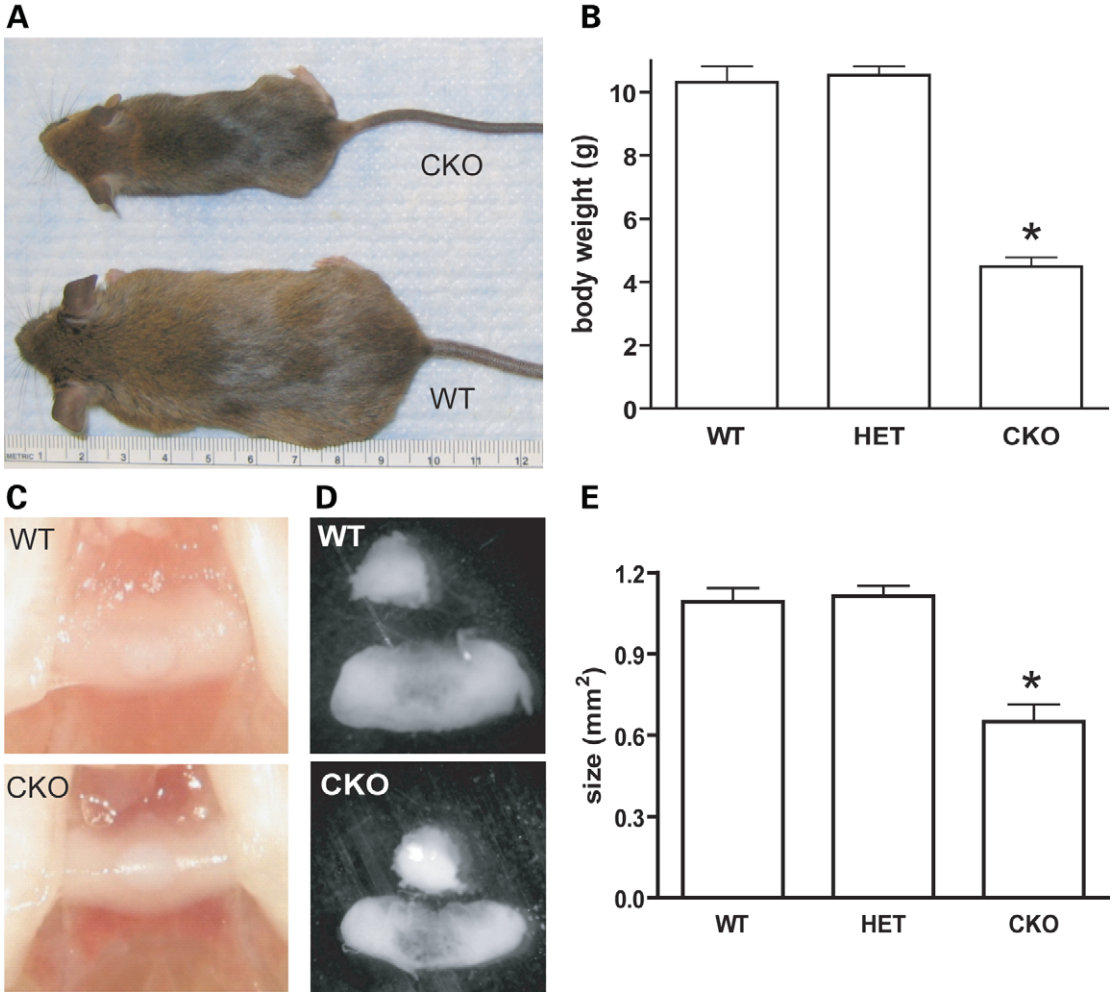

Figure 1. Decreased anterior pituitary size in *Nf1*^{BLBP}CKO (CKO) mice. (**A**) Postnatal growth was impaired in CKO mice resulting in proportionately smaller mice. (**B**) Body weights were significantly reduced in CKO, but not in BLBP-Cre; *Nf1*$^{flox/wt}$ (HET) or wild-type (WT), mice. (**C**) The entire pituitary gland appeared smaller in CKO mice *in situ*. Photomicrographs demonstrate the pituitary gland at the base of the skull. (**D**) Dissection of the pituitary gland revealed a disproportionate reduction in anterior pituitary size (lower image) with normal posterior pituitary size (upper image). (**E**) The surface area covered by the anterior lobe was significantly reduced in CKO mice. Asterisks denote statistically significant differences from control littermates ($P < 0.05$).

(Fig. 3F). The differential effect of neurofibromin loss on pituitary hormone production suggests that somatotropes and mammotropes are more severely affected by hypothalamic *Nf1* loss (27).

The early development of the hypothalamic–pituitary axis is orchestrated by a number of transcription factors. We selected a panel of these hypothalamic–pituitary axis transcriptional regulators (Ikaros1, Mash1, Math3 and Sox3) based on studies demonstrating that inactivation of these transcriptional regulation in mice leads to hypopituitary phenotypes similar to that observed in *Nf1*^{BLBP}CKO mice (28–31). Using qPCR, we found no differences in mRNA expression of these transcriptional factors in the postnatal *Nf1*^{BLBP}CKO hypothalamus compared with WT littermates (Supplementary Material, Fig. S3). These results suggest that neurofibromin loss does not cause pan-pituitary dysfunction, but rather leads to selective decreases in anterior pituitary GH and PRL production, and that these abnormalities do not reflect alterations in the expression of transcriptional factors important for normal hypothalamic–pituitary axis development.

The hypothalamic–pituitary abnormalities in *Nf1*^{BLBP}CKO mice are not recapitulated by Ras activation

Previous studies have shown that neurofibromin functions in part as a major negative regulator of Ras activity. To determine whether the increased Ras activation seen in the brains of *Nf1*^{BLBP}CKO mice accounted for the observed hypothalamic and pituitary abnormalities, we crossed BLBP-Cre mice with LSL-KRas^{G12D} mice (32) to generate mice with KRas activation in neural stem/progenitor cells. We chose to express KRas based on our observation that KRas is hyperactivated in *Nf1*-deficient neural stem cells and *Nf1*^{BLBP}CKO mouse brains (data not shown). In addition, activated KRas expression in GFAP+ cells of *Nf1*+/− mice resulted in optic gliomas, similar to *Nf1*+/− mice lacking neurofibromin expression in GFAP+ cells, while KRas hyperactivation in neural stem/progenitor cells (NSCs) produced an identical gliogenesis abnormality as neurofibromin loss in NSCs (11,18). In contrast to *Nf1*^{BLBP}CKO mice, BLBP-Cre; LSL-KRas^{G12D} (KRas*) mice did not display significant growth retardation (Fig. 4A). We found no significant

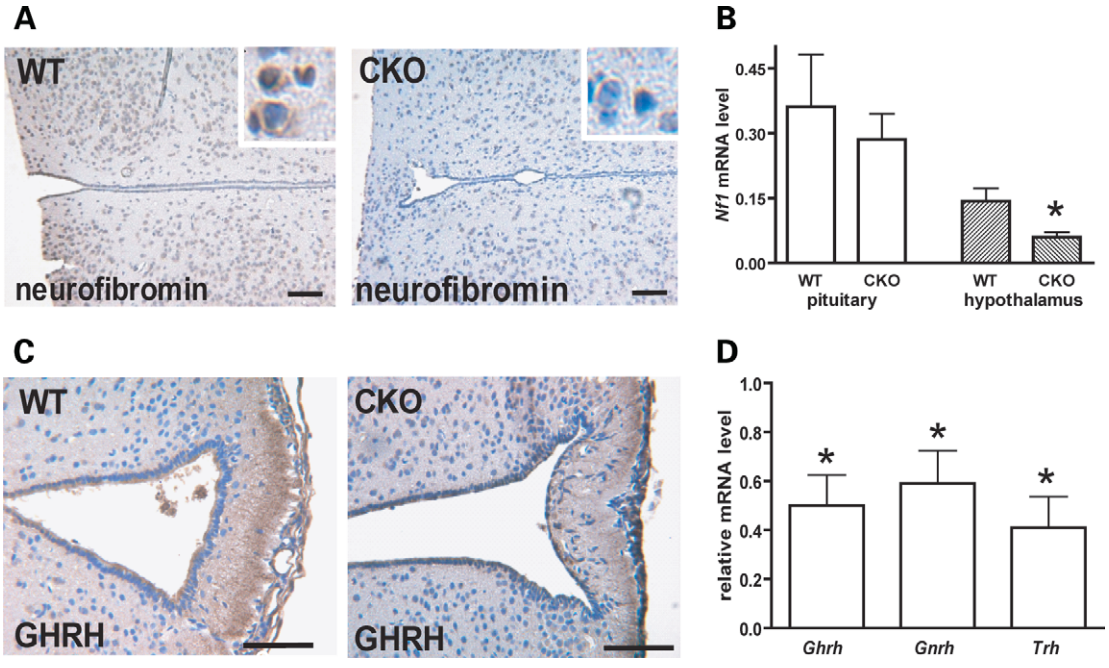

Figure 2. Hypothalamic loss of neurofibromin alters releasing hormone generation. (**A**) The number of neurofibromin-expressing cells was greatly reduced in the CKO hypothalamus. The inset shows individual labeled cells. (**B**) *Nf1* mRNA levels (normalized to *β-actin*) were lower in the hypothalamus, but not in the pituitary gland, of CKO mice as measured by quantitative real-time PCR. (**C**) GHRH immunolabeling was reduced in the median eminence of CKO mice. (**D**) *Ghrh*, *Gnrh* and *Trh* mRNA levels were reduced in the $Nf1^{BLBP}$CKO hypothalamus compared with littermate controls. Asterisks denote statistically significant differences from control littermates ($P < 0.05$). Scale bars, 100 μm, for the inset 10 μm.

decrease in pituitary gland size (Fig. 4B), pituitary cell proliferation (Fig. 4C) or *Ghrh* mRNA levels (Fig. 4D). Similarly, there was no growth retardation or impaired pituitary development in BLBP-Cre; LSL-myr-Akt mice that express a constitutively active form of Akt, an important downstream effector of Ras (data not shown). Collectively, these results indicate that the hypothalamic and pituitary abnormalities associated with neurofibromin loss in the brain are not Ras-dependent.

Expression of the neurofibromin GAP-related domain does not rescue the growth abnormalities seen in $Nf1^{BLBP}$CKO mice

Loss of neurofibromin results in Ras hyperactivation as well as increased activity of Ras downstream effectors, including Akt and Erk. Consistent with the role of neurofibromin as a Ras GTPase-activating protein, we observed a gene dose-dependent increase in the number of activated phospho-Erk1/2-labeled cells in hypothalamic tissue from $Nf1^{BLBP}$CKO mice at 2 weeks of age (Fig. 5A and B). However, despite the marked hyperactivation of these MAP kinases in the HET mice, there was no evidence of any growth retardation or hypothalamic abnormalities in these mice. These results are consistent with the above findings that KRas activation in neural stem/progenitor cells *in vivo* did not result in hypothalamic–pituitary or somatic growth defects. In light of previous studies in *Nf1*−/− cells showing that R-Ras activation leads to increased MAPK and Akt activation coupled with the results described above using KRas* and Akt* mice, it is unlikely that de-regulated Ras (or R-Ras) signaling accounts for the hypothalamic–pituitary axis and somatic growth abnormalities observed in $Nf1^{BLBP}$CKO mice.

Since mice with KRas or Akt activation do not exhibit abnormalities in hypothalamic–pituitary function, we next sought to determine whether expressing the Ras regulatory domain of neurofibromin *in vivo* would rescue the growth retardation observed in $Nf1^{BLBP}$CKO (CKO) mice. For these experiments, we bred $Nf1^{flox/flox}$ mice with Rosa-HA-GRD mice (33), which express the human GAP-related domain (GRD) from the Rosa promoter following Cre-mediated recombination. BLBP-Cre; $Nf1^{flox/wt}$ mice were then crossed with Rosa-HA-GRD; $Nf1^{flox/flox}$ mice to generate BLBP-Cre; Rosa-HA-GRD; $Nf1^{flox/flox}$ mice (CKO+GRD mice). As demonstrated by Epstein and coworkers (33), we similarly found that CKO + GRD mice had levels of Erk1/2 activation (surrogate marker of Ras activity) similar to WT mice (Fig. 6A), demonstrating that the Ras regulatory function of neurofibromin was restored by GRD expression. However, CKO + GRD mice exhibited the same smaller anterior pituitary sizes (data not shown), reduced body weights (Fig. 6B) and liver *Igf1* mRNA levels (Fig. 6C) as seen in their CKO littermates. Taken together, these results demonstrate that the growth abnormalities observed in $Nf1^{BLBP}$CKO mice are not dependent on neurofibromin Ras GAP function.

Molecular mechanism of neurofibromin-induced hypopituitarism

In addition to negatively regulating Ras activity, neurofibromin has been shown to positively regulate cAMP generation in the brain (16). Since Ras activation did not recapitulate

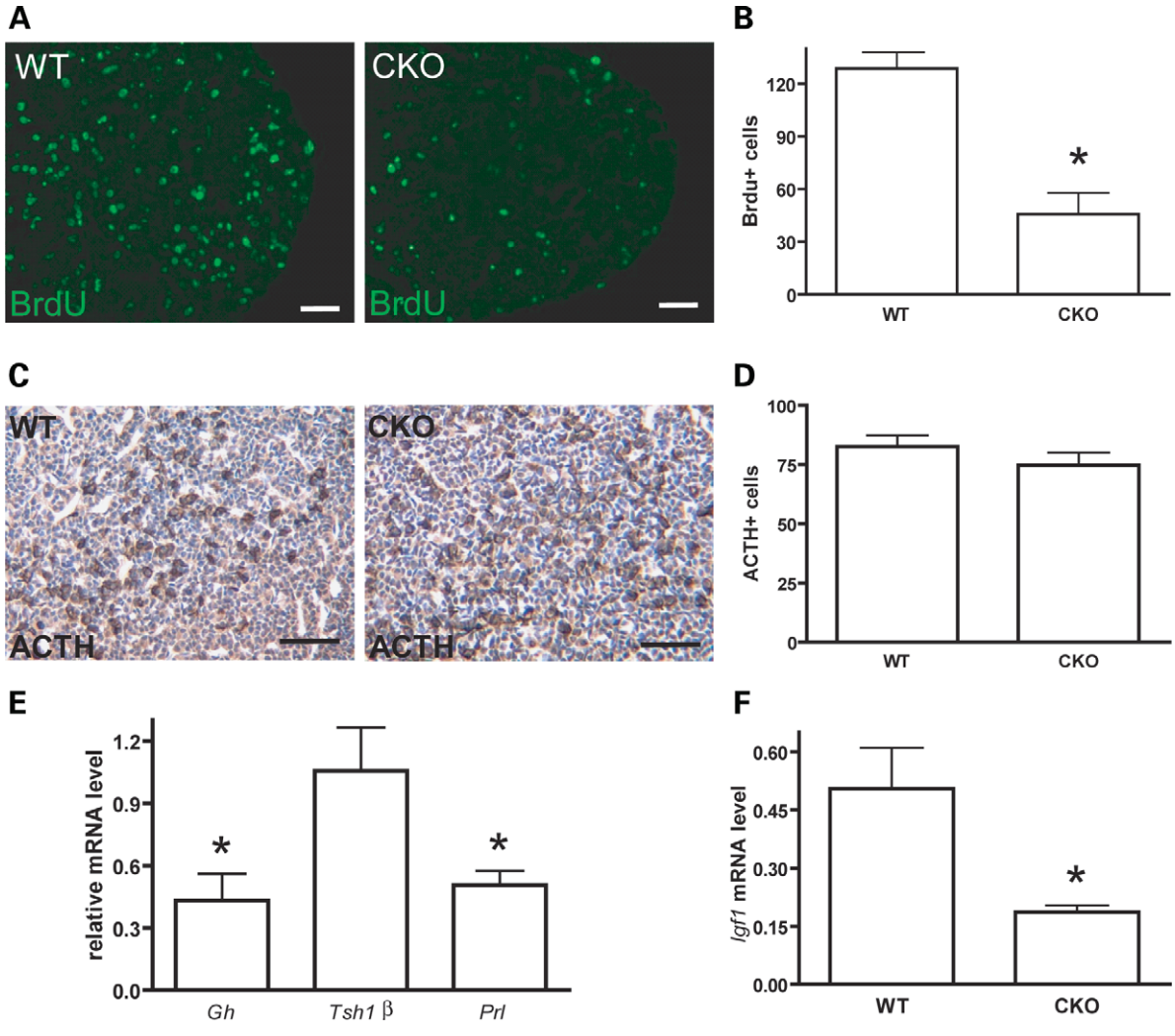

Figure 3. Impaired pituitary growth and hormone production. (**A**) Immunofluorescence detection of BrdU incorporation in the pituitary gland. (**B**) There was a significant reduction in the number of BrdU+ (proliferating) cells in the anterior pituitary. (**C**) ACTH immunohistochemistry showed normal labeling in CKO mice. (**D**) *Nf1* loss did not affect the number of ACTH+ cells. (**E**) GH and PRL mRNA levels were significantly reduced in the CKO mice, while *Tsh1*β mRNA levels were unchanged compared with WT controls. (**F**) *Igf1* mRNA levels were significantly lower in the livers of CKO mice. Asterisks denote statistically significant differences from control littermates ($P < 0.05$). Scale bars, 100 μm.

the hypothalamic or pituitary abnormalities observed in *Nf1*^{BLBP}CKO mice, we next sought to determine whether loss of neurofibromin alters cAMP levels in the hypothalamus. We observed a 50% decrease in the levels of cAMP in *Nf1*^{BLBP}CKO hypothalamic homogenates compared with littermate controls (Fig. 7A). These reduced cAMP levels were associated with decreased activation of the cAMP responsive transcription factor, CREB. In this regard, we have previously shown that PN1 *Nf1*^{BLBP}CKO mice exhibit decreased hypothalamic CREB activation (18). Consistent with these findings, loss of CREB expression in the developing CNS leads to decreased GHRH release from hypothalamic neurons and subsequently causes hypopituitarism (34).

In order to increase cAMP levels in *Nf1*^{BLBP}CKO mice *in vivo*, we administered rolipram, a specific phosphodiesterase-4 inhibitor (35). Rolipram has been shown to elevate CREB activation in the brain following intraperitoneal delivery (36). For these experiments, rolipram was injected daily from E11.5 to PN18 to timed-pregnant dams and to their pups from PN7 through PN18. We have previously shown that rolipram injection partially restored cAMP levels in the forebrains of *Nf1*^{BLBP}CKO mice and corrected the cortical thickness defect associated with *Nf1* loss (18). Following rolipram treatment of *Nf1*^{BLBP}CKO mice, there was a significant increase in body weight compared with untreated age-matched *Nf1*^{BLBP}CKO mice at 2 weeks of age; however, the rolipram-injected mice were still smaller than littermate controls (Fig. 7B). In contrast, rolipram had no effect on the weights of WT or HET mice. The fact that inhibition of phosphodiesterase activity partially rescues the phenotype is consistent with previous studies demonstrating that neurofibromin increases the production of cAMP by activating adenylyl cyclase (14,16), and that forskolin, an adenylyl cyclase activator, stimulates the release of GHRH in a

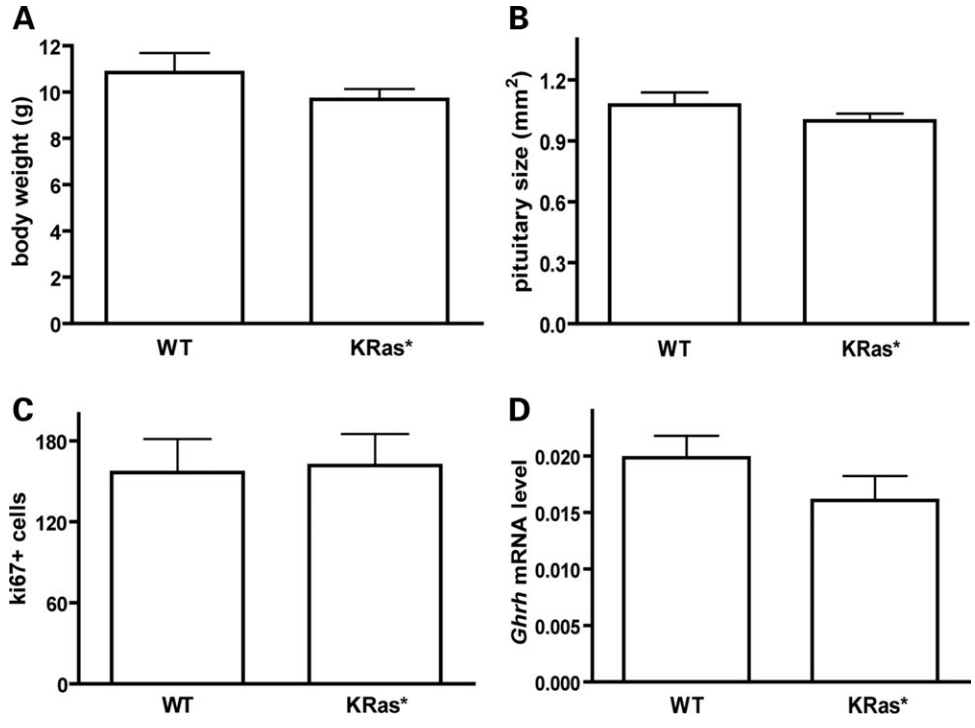

Figure 4. Constitutive activation KRas does not impair somatic growth. (**A**) The modest decrease in body weights of BLBP-Cre; LSL-KRas (KRas*) mice was not statistically significant. (**B**) No significant change in the surface area of the anterior pituitary was seen in KRas* mice. (**C**) The number of Ki67-labeled nuclei was unchanged in KRas* mice. (**D**) The slight reduction in *Ghrh* levels in the hypothalamus was not statistically significant, as determined by qPCR. Asterisks denote statistically significant differences from control littermates ($P < 0.05$).

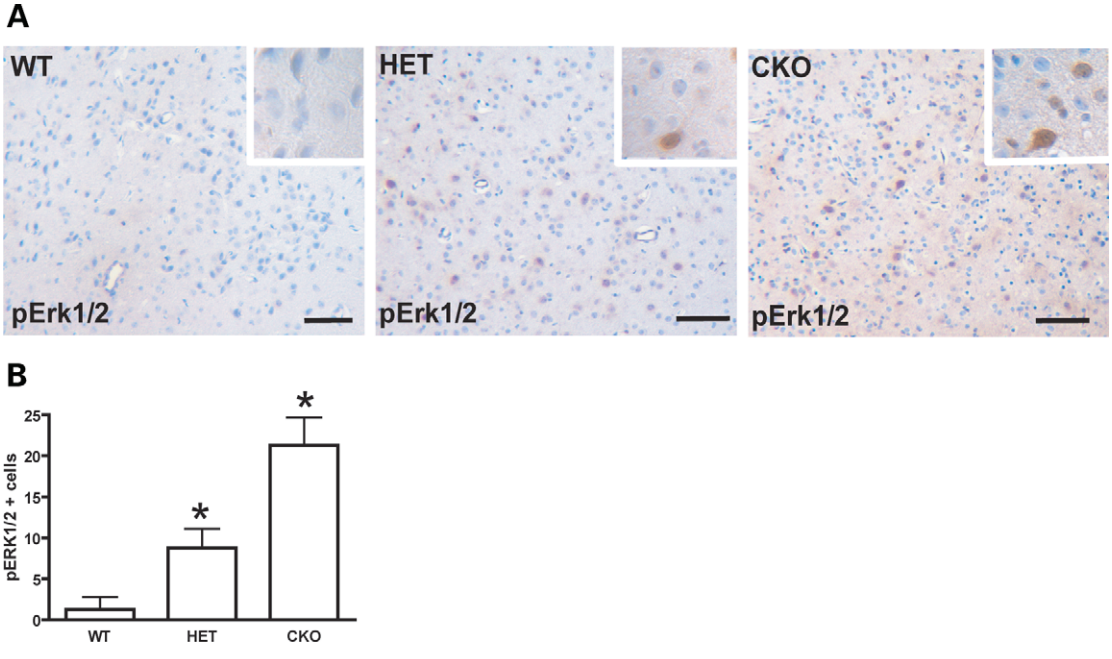

Figure 5. Erk activation does not correlate with the somatic growth defects in *Nf1*^{BLBP}CKO mice. (**A**) Increased activation of Erk1/2 was observed in the hypothalamus from both HET and CKO mice compared with WT controls. The inset shows individual labeled cells. (**B**) There was a significant gene dose-dependent increase in the number of phospho-Erk1/2 labeled cells in the hypothalamus. Scale bars, 100 μm, for the inset 30 μm.

concentration-dependent fashion (37). Moreover, the magnitude of the body weight rescue following rolipram treatment (∼50%) is similar to that observed following PKA expression in *Nf1*−/− *Drosophila* (19).

DISCUSSION

One common feature of individuals with NF1 is relatively short stature compared with their unaffected siblings. The

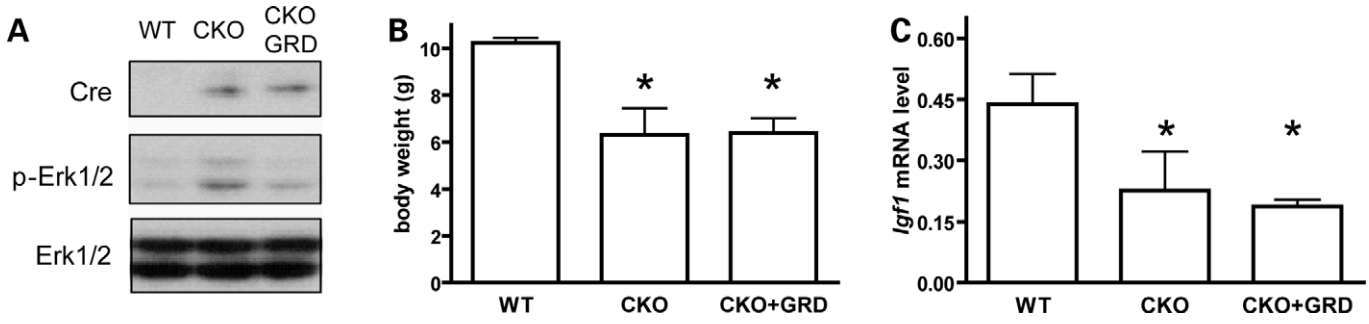

Figure 6. Expression of the neurofibromin GAP-related domain (GRD) does not rescue the reduced growth or *Igf*-1 mRNA levels seen in CKO mice. (**A**) *NF1*-GRD expression in *Nf1*^{BLBP}CKO mice (CKO GRD) restored Erk1/2 activation (phospho-Erk1/2; p-Erk1/2) to WT levels. (**B**) In contrast, GRD expression had no effect on body weight (CKO+GRD mice) compared with CKO littermates. (**C**) Liver *Igf1* mRNA levels were also not changed by GRD expression. Asterisks denote statistically significant differences from control littermates ($P < 0.05$).

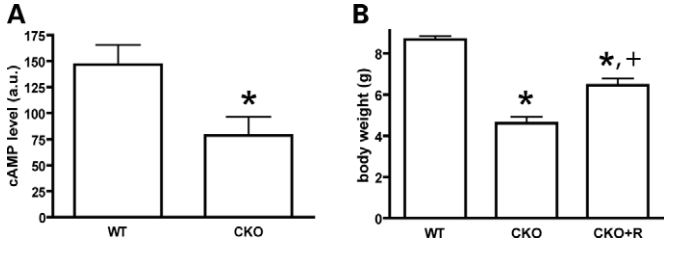

Figure 7. Cyclic AMP levels, but not Erk activation, correlates with the somatic growth defects in *Nf1*^{BLBP}CKO mice. (**A**) Cyclic AMP levels, as measured by enzyme immunoassay, were significantly lower in the hypothalamus of CKO mice. (**B**) Daily rolipram treatment partially restored the somatic growth defect. At 2 weeks of age, both the untreated and the rolipram-injected CKO mice were significantly smaller than their WT littermates ($P < 0.005$; asterisks); however, rolipram treatment significantly increased the body weights of *Nf1*^{BLBP}CKO mice ($P = 0.01$; '†').

observation that some of these children have either subclinical or overt GH deficiency prompted us to examine somatic growth in a recently developed *Nf1* mutant mouse. In the present study, we demonstrate that neurofibromin regulates the function of the hypothalamic–pituitary axis and that *Nf1* loss in the brain leads to decreased GH and IGF levels.

Previous studies of *Nf1*-deficient *Drosophila* have similarly shown that neurofibromin regulates growth at the organismal level (19), and have implicated a select neuronal population in the developing larval CNS (20,38). Consistent with the idea that the growth defect may reflect the impact of neurofibromin loss on neurons, growth deficits have also been observed in mice with neuron-specific conditional *Nf1* inactivation (39). Using the synapsin-1 promoter to induce loss of neurofibromin expression in neurons by E12.5, growth retardation becomes evident in these *Nf1*^{Syn1}CKO mice by PN3-4, analogous to what we observed in *Nf1*^{BLBP}CKO mice. In addition, dwarfism has similarly been reported in mice in which neurofibromin loss occurs in neuroglial progenitors by E11.5 (40). These mice exhibit both neuronal and astroglial cell loss of neurofibromin, and demonstrate a significant reduction in body weight by PN8. In contrast, mice with predominantly glial *Nf1* inactivation (41) had normal body weights and sizes (Supplementary Material, Fig. S2A). Furthermore, in these mice, we observed no significant changes in hypothalamic GHRH expression or liver *Igf1* expression (Supplementary Material, Fig. S2B). Together, these findings suggest that the growth retardation observed in *Nf1* mutant mice and flies is the result of a primary neuronal defect.

Neurofibromin regulates the development of the nervous system in both a Ras- and cAMP-dependent fashion. Loss of neurofibromin results in the expansion of glial cell populations as a consequence of de-regulated Ras signaling in *Nf1* mutant mice (11). We have recently shown that activation of either Ras or Akt in neural progenitor cells is sufficient to recapitulate the glial abnormalities observed in *Nf1*^{BLBP}CKO mice, whereas increasing cAMP levels by inhibiting phosphodiesterase activity in the developing brain fails to ameliorate this glial abnormality (18). In contrast, neurofibromin regulates neuronal maturation through Ras-independent mechanisms. In this regard, *Nf1* inactivation in neural progenitors or neurons results in decreased cortical thickness *in vivo* (18,39), which we have recently shown reflects reduced neurite lengths *in vitro* and *in vivo*. Importantly, the cortical thickness and neurite length phenotypes were not recapitulated by constitutive activation of KRas or Akt, but were restored by increasing cAMP levels *in vitro* and *in vivo* (18). Collectively, these findings suggest that neurofibromin regulates neuronal differentiation by modulating cAMP levels.

Cyclic AMP and the transcription factor cAMP response element binding protein (CREB) are critical regulators of hypothalamic–pituitary axis development. A number of key transcription factors and hormones expressed in the pituitary gland have CREB binding sites in their promoter regions (42,43). The physiological importance of cAMP signaling and CREB activation in the regulation of pituitary GH production has been elegantly demonstrated using several genetically engineered mouse strains: Mice with *Gh* promoter-driven expression of a non-phosphorylatable CREB have decreased CREB activity, resulting in dwarfism (44). The reduced body size in these CREBM1 transgenic mice reflects atrophy of the anterior pituitary without any effects on the intermediate or posterior pituitary. In contrast, *Gh* promoter-mediated expression of cholera toxin caused increased cAMP levels and led to pituitary hyperplasia and gigantism in mice (45). These transgenic mice had significantly larger body weights and high levels of circulating GH.

The importance of CREB signaling in hypothalamic–pituitary axis function and short stature is further underscored

by the identification of mutations in the CREB binding protein CBP in Rubinstein–Taybi syndrome. Similar to children with NF1, children with Rubinstein–Taybi syndrome have poor growth during the first few months of life, resulting in short stature (46). In addition, mice expressing a truncated CBP gene exhibit growth retardation (47). Of note, GH deficiency has also been reported in some cases of Rubinstein–Taybi syndrome (48).

In addition, cAMP and CREB are major regulators of hypothalamic development. *In vitro*, cAMP modulates the functional development of hypothalamic neurons (49). In these studies, forskolin treatment produced similar effects as cholera toxin, suggesting that cAMP was critical for hypothalamic neuronal maturation. Similarly, rolipram treatment significantly increased the length of dendrites in hippocampal neurons *in vivo* (36). Forskolin and cAMP analogs also increase neurite extension and functional maturation in hypothalamic neurons *in vitro* (50). These observations are consistent with our findings that forskolin treatment reversed the *Nf1*-deficient neuronal neurite length defect *in vitro* and that increasing brain cAMP levels by rolipram treatment resulted in a partial rescue of the growth retardation phenotype *in vivo* (18).

The importance of CREB in hypothalamic function is underscored by the following observations: First, CREB mediates developmental gap junction uncoupling during the postnatal development of hypothalamic neurons *in vitro* (51). These gap junctions act as electrical synapses and allow cAMP and other signaling molecules to coordinate transcriptional activities in developing hypothalamic neurons. Second, brain-specific loss of CREB results in hypopituitarism and dwarfism (34). While CREB is normally expressed in the pituitary glands of these mice, the lack of CREB activity in the hypothalamus resulted in a robust decrease in GHRH release into the portal system of the median eminence. Similar to $Nf1^{BLBP}$CKO mice, *Creb*-deficient mice had body weight reductions which reached statistical significance at PN8.

Genetically engineered *Nf1* mouse models have already begun to provide fundamentally important insights into the pathogenesis of numerous NF1-associated phenotypes, including plexiform neurofibroma (52), optic glioma (53), leukemia (54) and malignant peripheral nerve sheath tumors (55,56) as well as non-neoplastic features, such as bone and vascular abnormalities (57,58). The $Nf1^{BLBP}$CKO mouse model described herein was used to identify an understudied abnormality in children with NF1. Given the lack of autopsy studies on NF1 patient brains, limited information is available about the structure or composition of the hypothalamus and pituitary gland in individuals with NF1. However, using $Nf1^{BLBP}$CKO mice, we found that somatic growth resulting from hypothalamic–pituitary dysfunction reflects abnormal Ras-independent signaling resulting from *Nf1* inactivation in neural progenitors. These findings have relevance to the human condition in that they uncover a responsible signaling pathway and suggest that future studies might measure circulating IGF1 or GH levels in children with NF1 to identify subclinical hypothalamic–pituitary dysfunction.

Interestingly, despite the reduced body weights and organ sizes, the brain weights of $Nf1^{BLBP}$CKO mice are unchanged. These disproportional changes result in relative megalencephaly, similar to what has been reported for children with NF1 (1,59). The relative megalencephaly could reflect increased numbers of glial precursors, oligodendrocytes or astrocytes (18). In support of this hypothesis, magnetic resonance imaging studies have found increases in both grey and white matter volumes in the brains of children with NF1 (60–62).

Collectively, these data demonstrate for the first time that neurofibromin regulates hypothalamic function and pituitary development in the mammalian CNS by modulating intracellular cAMP levels. The observation that *Nf1* inactivation in neural progenitor cells results in decreased GH and IGF1 levels is exciting in light of the short stature seen in individuals affected with NF1. Finally, the finding that neurofibromin regulates hypothalamic and pituitary function in part by controlling cAMP levels offers unique insights into the mechanisms underlying NF1-associated growth abnormalities and may lead to future therapies that target this neurofibromin-regulated pathway.

MATERIALS AND METHODS

Mice and tissue preparation

BLBP-Cre transgenic mice were successively intercrossed with $Nf1^{flox/flox}$ mice (39) to generate BLBP-Cre; $Nf1^{flox/flox}$ ($Nf1^{BLBP}$CKO or 'CKO') mice. BLBP-Cre mice were also crossed with Lox-stop-lox (LSL)-$KRas^{G12D}$ or Lox-stop-lox (LSL)-myr-Akt mice to generate BLBP-Cre; LSL-$KRas^{G12D}$ ($KRas^{*}$) or BLBP-Cre; LSL-myr-Akt mice (Akt^{*}), respectively. Rosa-GRD (33) mice were bred with $Nf1^{flox/flox}$ and subsequently with BLBP-Cre; $Nf1^{flox/wt}$ mice in order to generate BLBP-Cre; Rosa-GRD;$Nf1^{flox/flox}$ (CKO+GRD). All strains were maintained on a C57BL/6 background and used in accordance with established and approved mouse protocols at Washington University.

PN18 mice were intraperitoneally injected with BrdU 3 h prior to euthanasia. Mice were perfused transcardially with PBS. A small portion of the liver was removed and snap-frozen before perfusion with 4% PFA in PBS. Following overnight post-fixation at 4°C, the pituitary glands and 2 mm brain slices were transferred to 70% ethanol solution prior to paraffin embedding and sectioning. For RNA preparation, mice were terminally anaesthetized and the brains and pituitary glands were quickly removed, dissected and snap frozen.

Pituitary size measurement

The dissected pituitary glands were photographed under a dissecting microscope and the entire pituitary gland as well as the posterior pituitary was manually circumscribed and the area determined using SysImage (Soft Imaging System, Lakewood, CO) image analysis software (Supplementary Material, Fig. S1). The anterior pituitary area was estimated by subtracting the posterior pituitary area from the size of the entire pituitary gland. For each genotype, four dissected pituitary glands were measured from 18-day-old mice of both sexes. WT and heterozygous littermates were included for comparison.

Immunohistochemistry

Five-micron paraffin sections were deparaffinized, treated for citrate antigen retrieval and incubated in 5% serum blocking solution prior to the overnight incubation of primary antibodies at 4°C for 18 h. ACTH, GHRH and Ki67 antibodies were purchased from Peninsula Lab (San Carlos, CA), Abcam (Cambridge, MA) and BD Pharmingen (San Jose, CA), respectively. Antibodies against phospho-CREB and phospho-Erk1/2 were obtained from Cell Signaling Technology, Danvers, MA. Horseradish peroxidase-conjugated secondary antibodies (Vector Laboratories, Burlingame, CA) were incubated for 1 h at room temperature (RT) and Vectastain Elite ABC development was employed as previously published. Sections were then counterstained with hematoxylin. For BrdU labeling, deparaffinized sections were treated with 0.1% trypsin in PBS for 10 min at RT. DNA was denatured by 0.1 M HCl for 10 min at 4°C and 4 M HCl for 30 min at 37°C followed by two rinses of 0.1 M boric acid (pH = 8.0) for 5 min at RT prior to blocking. The primary anti- BrdU antibody (Abcam) was applied overnight at 4°C and fluorescent detection was performed with Alexa 488-labeled secondary antibody (Molecular Probes, Eugene, OR) for 60 min at RT. TUNEL labeling on the paraffin sections was performed according to the manufacturer's instructions (Roche Diagnostics, Nutley, NJ). The number of BrdU- and ACTH-immunoreactive cells as well as of TUNEL-positive cells in the sections were quantified by direct counting on two non-consecutive sections for at least three mice in each genotype.

Real-time reverse transcription PCR

Snap frozen tissues (liver, pituitary gland, hypothalamus and brain) were homogenized in TRIzol reagent (Invitrogen, Carlsbad, CA) to extract total RNA. Two micrograms of total RNA extracted from each sample were used to make cDNA. Thirty nanograms of cDNA were used as a template for the determination of the transcription of specific genes by real-time PCR (RT-PCR) using SYBR® Green detection and transcript specific primers. The primers used were: *Nf1* sense (5′ AAT CAG TGG TTA GCC AGC GC 3′), *Nf1* antisense (5′ TTC ATA CGG CGA GAC AAT GG 3′); *Gh* sense (5′ TTC CAT TCA GAA TGC CCA GG 3′), *Gh* antisense (5′ CGA AGC AAT TCC ATG TCG GT 3′); *Igf1* sense (5′ GCT GCA AAG GAG AAG GAA AGG 3′), *Igf1* antisense (5′ TGG CAT TTT CTG CTC CGT G 3′); *Tsh1β* sense (5′ GCA GCA TCC TTT TGT ATT CCC 3′), *Tsh1β* antisense (5′ CCG TGT CAT ACA ATA CCC AGC 3′); *GHRH* sense (5′ GCT GTA TGC CCG GAA AGT GAT 3′), *Ghrh* antisense (5′ AAT CCC TGC AAG ATG CTC TCC 3′); *Trh* sense (5′ GAG GAA GAC GTT GAA GCC GAA 3′), *TRH* antisense (5′ ATC CTT GTC TTG GTT GGC ACG 3′); *Gnrh* sense (5′ TGT GTG TTT GGA AGG CTG CTC 3′) and *Gnrh* antisense (5′ CCT TGC CCA TCT CTT GGA AAG 3′); *Ikaros1* sense (5′ AGC ACA GCA GAA CTC CAA GAG TGA 3′) and *Ikaros1* antisense (5′ TTC ATT TCA CAG GCA CGC CCA TTC 3′); *Mash1* sense (5′ ACG ACT TGA ACT CTA TGG CGG GTT 3′) and *Mash1* antisense (5′ AAG TCC AGC AGC TCT TGT TCC TCT 3′); *Math3* sense (5′ AGG AAC TAC ATC TGG GCC TTG TCT 3′) and *Math3* antisense (5′ TGC TTG TGG GTT GAG AGA GAC CTT 3′); *Sox3* sense (5′ ACT GGA AAC TGC TGA CCG ATG 3′) and *Sox3* antisense (5′ TGT CCT TCT TGA GCA GCG TCT 3′). PCR reactions without cDNA samples were used as negative controls. Each reaction was performed in duplicate. The fluorescent data were converted into cycle threshold (CT) measurements, and the ΔΔCT method was used to calculate fold expression relative to littermate control samples, using β-actin as an internal control.

Cyclic AMP measurements

Dissected hypothalamic regions of brains were snap-frozen in liquid nitrogen, triturated in ice-cold 5% trichloroacetic acid (10 μl per mg tissue) and centrifuged at 1000*g* for 10 min at 4°C. Supernatants supplemented with equal volume of 0.1 M HCl were extracted with water-saturated ether thrice prior to desiccation in a vacuum centrifuge. The cAMP content was determined using a cyclic AMP enzyme immunoassay kit (Assay Designs, Ann Arbor, MI).

Statistical analysis

Each experiment was performed with samples from at least three mice for each genotype or treatment condition. Statistical significance ($P < 0.05$) was determined by paired or unpaired *t*-test (with Welch's Correction) using GraphPad Prism 4.0 software (GraphPad Inc., San Diego, CA).

SUPPLEMENTARY MATERIAL

Supplementary Material is available at HMG Online.

FUNDING

This work was supported by grants from the National Cancer Institute Mouse Models of Human Cancers Consortium and Department of Defense to D.H.G. B.H. was supported by a nested post-doctoral fellowship from the Department of Defense.

ACKNOWLEDGEMENTS

We thank Scott Gianino and Scott Bahr for expert technical assistance. We also thank Drs Luis Parada, Tyler Jacks, Jonathan Epstein and Ernesto Bernal-Mizrachi for generously providing the *Nf1*$^{flox/flox}$, LSL-KRas^{G12D}, Rosa-HA-GRD and LSL-myr-Akt1 mice, respectively. We appreciate the helpful discussions provided by Dr Louis Muglia during the preparation of this manuscript.

Conflict of Interest statement. None declared.

REFERENCES

1. Szudek, J., Birch, P. and Friedman, J.M. (2000) Growth in North American white children with neurofibromatosis 1 (NF1). *J. Med. Genet.*, **37**, 933–938.
2. Virdis, R., Street, M.E., Bandello, M.A., Tripodi, C., Donadio, A., Villani, A.R., Cagozzi, L., Garavelli, L. and Bernasconi, S. (2003)

Growth and pubertal disorders in neurofibromatosis type 1. *J. Pediatr. Endocrinol. Metab.*, **16** (Suppl. 2), 289–292.
3. Zeitlhuber, U., Frisch, H., Toifl, K. and Wimmer, S. (1984) Hormonal findings in children with central manifestations of Recklinghausen's neurofibromatosis. *Klin. Padiatr.*, **196**, 14–17.
4. Vassilopoulou-Sellin, R., Klein, M.J. and Slopis, J.K. (2000) Growth hormone deficiency in children with neurofibromatosis type 1 without suprasellar lesions. *Pediatr. Neurol.*, **22**, 355–358.
5. DeClue, J.E., Papageorge, A.G., Fletcher, J.A., Diehl, S.R., Ratner, N., Vass, W.C. and Lowy, D.R. (1992) Abnormal regulation of mammalian p21ras contributes to malignant tumor growth in von Recklinghausen (type 1) neurofibromatosis. *Cell*, **69**, 265–273.
6. Xu, G.F., O'Connell, P., Viskochil, D., Cawthon, R., Robertson, M., Culver, M., Dunn, D., Stevens, J., Gesteland, R., White, R. *et al.* (1990) The neurofibromatosis type 1 gene encodes a protein related to GAP. *Cell*, **62**, 599–608.
7. Ballester, R., Marchuk, D., Boguski, M., Saulino, A., Letcher, R., Wigler, M. and Collins, F. (1990) The NF1 locus encodes a protein functionally related to mammalian GAP and yeast IRA proteins. *Cell*, **63**, 851–859.
8. Martin, G.A., Viskochil, D., Bollag, G., McCabe, P.C., Crosier, W.J., Haubruck, H., Conroy, L., Clark, R., O'Connell, P., Cawthon, R.M. *et al.* (1990) The GAP-related domain of the neurofibromatosis type 1 gene product interacts with ras p21. *Cell*, **63**, 843–849.
9. Bollag, G., Clapp, D.W., Shih, S., Adler, F., Zhang, Y.Y., Thompson, P., Lange, B.J., Freedman, M.H., McCormick, F., Jacks, T. *et al.* (1996) Loss of NF1 results in activation of the Ras signaling pathway and leads to aberrant growth in haematopoietic cells. *Nat. Genet.*, **12**, 144–148.
10. Lau, N., Feldkamp, M.M., Roncari, L., Loehr, A.H., Shannon, P., Gutmann, D.H. and Guha, A. (2000) Loss of neurofibromin is associated with activation of RAS/MAPK and PI3-K/AKT signaling in a neurofibromatosis 1 astrocytoma. *J. Neuropathol. Exp. Neurol.*, **59**, 759–767.
11. Dasgupta, B., Li, W., Perry, A. and Gutmann, D.H. (2005) Glioma formation in neurofibromatosis 1 reflects preferential activation of K-RAS in astrocytes. *Cancer Res.*, **65**, 236–245.
12. Hiatt, K.K., Ingram, D.A., Zhang, Y., Bollag, G. and Clapp, D.W. (2001) Neurofibromin GTPase-activating protein-related domains restore normal growth in Nf1−/− cells. *J. Biol. Chem.*, **276**, 7240–7245.
13. Thomas, S.L., Deadwyler, G.D., Tang, J., Stubbs, E.B., Jr, Muir, D., Hiatt, K.K., Clapp, D.W. and De Vries, G.H. (2006) Reconstitution of the NF1 GAP-related domain in NF1-deficient human Schwann cells. *Biochem. Biophys. Res. Commun.*, **348**, 971–980.
14. Dasgupta, B., Dugan, L.L. and Gutmann, D.H. (2003) The neurofibromatosis 1 gene product neurofibromin regulates pituitary adenylate cyclase-activating polypeptide-mediated signaling in astrocytes. *J. Neurosci.*, **23**, 8949–8954.
15. Guo, H.F., The, I., Hannan, F., Bernards, A. and Zhong, Y. (1997) Requirement of Drosophila NF1 for activation of adenylyl cyclase by PACAP38-like neuropeptides. *Science*, **276**, 795–798.
16. Tong, J., Hannan, F., Zhu, Y., Bernards, A. and Zhong, Y. (2002) Neurofibromin regulates G protein-stimulated adenylyl cyclase activity. *Nat. Neurosci.*, **5**, 95–96.
17. Warrington, N.M., Woerner, B.M., Daginakatte, G.C., Dasgupta, B., Perry, A., Gutmann, D.H. and Rubin, J.B. (2007) Spatiotemporal differences in CXCL12 expression and cyclic AMP underlie the unique pattern of optic glioma growth in neurofibromatosis type 1. *Cancer Res.*, **67**, 8588–8595.
18. Hegedus, B., Dasgupta, B., Shin, J., Emnett, R., Hart-Mahon, E., Elghazi, L., Bernal-Mizrachi, E. and Gutmann, D.H. (2007) Neurofibromatosis-1 regulates neuronal and glial cell differentiation from neuroglial progenitors *in vivo* by both cAMP- and Ras-dependent mechanisms. *Cell Stem Cell*, **1**, 443–457.
19. The, I., Hannigan, G.E., Cowley, G.S., Reginald, S., Zhong, Y., Gusella, J.F., Hariharan, I.K. and Bernards, A. (1997) Rescue of a Drosophila NF1 mutant phenotype by protein kinase A. *Science*, **276**, 791–794.
20. Walker, J.A., Tchoudakova, A.V., McKenney, P.T., Brill, S., Wu, D., Cowley, G.S., Hariharan, I.K. and Bernards, A. (2006) Reduced growth of Drosophila neurofibromatosis 1 mutants reflects a non-cell-autonomous requirement for GTPase-Activating Protein activity in larval neurons. *Genes Dev.*, **20**, 3311–3323.
21. Huang, Y., Rangwala, F., Fulkerson, P.C., Ling, B., Reed, E., Cox, A.D., Kamholz, J. and Ratner, N. (2004) Role of TC21/R-Ras2 in enhanced migration of neurofibromin-deficient Schwann cells. *Oncogene*, **23**, 368–378.
22. Elghazi, L., Weiss, A.J., Gould, A.P., Hegedus, B., Gutmann, D.H. and Bernal-Mizrachi, E. (2008) Generation of a reporter mouse line expressing Akt and EGFP upon Cre-mediated recombination. *Genesis*, **46**, 256–264.
23. Frohman, L.A. and Kineman, R.D. (2002) Growth hormone-releasing hormone and pituitary development, hyperplasia and tumorigenesis. *Trends Endocrinol. Metab.*, **13**, 299–303.
24. Li, H., Zeitler, P.S., Valerius, M.T., Small, K. and Potter, S.S. (1996) Gsh-1, an orphan Hox gene, is required for normal pituitary development. *EMBO J*, **15**, 714–724.
25. Flavell, D.M., Wells, T., Wells, S.E., Carmignac, D.F., Thomas, G.B. and Robinson, I.C. (1996) Dominant dwarfism in transgenic rats by targeting human growth hormone (GH) expression to hypothalamic GH-releasing factor neurons. *EMBO J.*, **15**, 3871–3879.
26. Godfrey, P., Rahal, J.O., Beamer, W.G., Copeland, N.G., Jenkins, N.A. and Mayo, K.E. (1993) GHRH receptor of little mice contains a missense mutation in the extracellular domain that disrupts receptor function. *Nat. Genet.*, **4**, 227–232.
27. Luque, R.M., Amargo, G., Ishii, S., Lobe, C., Franks, R., Kiyokawa, H. and Kineman, R.D. (2007) Reporter expression, induced by a growth hormone promoter-driven Cre recombinase (rGHp-Cre) transgene, questions the developmental relationship between somatotropes and lactotropes in the adult mouse pituitary gland. *Endocrinology*, **148**, 1946–1953.
28. Ezzat, S., Mader, R., Fischer, S., Yu, S., Ackerley, C. and Asa, S.L. (2006) An essential role for the hematopoietic transcription factor Ikaros in hypothalamic-pituitary-mediated somatic growth. *Proc. Natl Acad. Sci. USA*, **103**, 2214–2219.
29. Rizzoti, K., Brunelli, S., Carmignac, D., Thomas, P.Q., Robinson, I.C. and Lovell-Badge, R. (2004) SOX3 is required during the formation of the hypothalamo-pituitary axis. *Nat. Genet.*, **36**, 247–255.
30. Zhu, X., Zhang, J., Tollkuhn, J., Ohsawa, R., Bresnick, E.H., Guillemot, F., Kageyama, R. and Rosenfeld, M.G. (2006) Sustained Notch signaling in progenitors is required for sequential emergence of distinct cell lineages during organogenesis. *Genes Dev.*, **20**, 2739–2753.
31. Tomita, K., Moriyoshi, K., Nakanishi, S., Guillemot, F. and Kageyama, R. (2000) Mammalian achaete-scute and atonal homologs regulate neuronal versus glial fate determination in the central nervous system. *EMBO J.*, **19**, 5460–5472.
32. Johnson, L., Mercer, K., Greenbaum, D., Bronson, R.T., Crowley, D., Tuveson, D.A. and Jacks, T. (2001) Somatic activation of the K-ras oncogene causes early onset lung cancer in mice. *Nature*, **410**, 1111–1116.
33. Ismat, F.A., Xu, J., Lu, M.M. and Epstein, J.A. (2006) The neurofibromin GAP-related domain rescues endothelial but not neural crest development in Nf1 mice. *J. Clin. Invest.*, **116**, 2378–2384.
34. Mantamadiotis, T., Kretz, O., Ridder, S., Bleckmann, S.C., Bock, D., Grone, H.J., Malaterre, J., Dworkin, S., Ramsay, R.G. and Schutz, G. (2006) Hypothalamic 3′,5′-cyclic adenosine monophosphate response element-binding protein loss causes anterior pituitary hypoplasia and dwarfism in mice. *Mol. Endocrinol.*, **20**, 204–211.
35. Barad, M., Bourtchouladze, R., Winder, D.G., Golan, H. and Kandel, E. (1998) Rolipram, a type IV-specific phosphodiesterase inhibitor, facilitates the establishment of long-lasting long-term potentiation and improves memory. *Proc. Natl Acad. Sci. USA*, **95**, 15020–15025.
36. Fujioka, T., Fujioka, A. and Duman, R.S. (2004) Activation of cAMP signaling facilitates the morphological maturation of newborn neurons in adult hippocampus. *J. Neurosci.*, **24**, 319–328.
37. Cugini, C.D., Jr, Millard, W.J. and Leidy, J.W., Jr (1991) Signal transduction systems in growth hormone-releasing hormone and somatostatin release from perifused rat hypothalamic fragments. *Endocrinology*, **129**, 1355–1362.
38. Hannan, F., Ho, I., Tong, J.J., Zhu, Y., Nurnberg, P. and Zhong, Y. (2006) Effect of neurofibromatosis type I mutations on a novel pathway for adenylyl cyclase activation requiring neurofibromin and Ras. *Hum. Mol. Genet.*, **15**, 1087–1098.
39. Zhu, Y., Romero, M.I., Ghosh, P., Ye, Z., Charnay, P., Rushing, E.J., Marth, J.D. and Parada, L.F. (2001) Ablation of NF1 function in neurons induces abnormal development of cerebral cortex and reactive gliosis in the brain. *Genes Dev.*, **15**, 859–876.
40. Zhu, Y., Harada, T., Liu, L., Lush, M.E., Guignard, F., Harada, C., Burns, D.K., Bajenaru, M.L., Gutmann, D.H. and Parada, L.F. (2005)

Inactivation of NF1 in CNS causes increased glial progenitor proliferation and optic glioma formation. *Development*, **132**, 5577–5588.
41. Bajenaru, M.L., Zhu, Y., Hedrick, N.M., Donahoe, J., Parada, L.F. and Gutmann, D.H. (2002) Astrocyte-specific inactivation of the neurofibromatosis 1 gene (NF1) is insufficient for astrocytoma formation. *Mol. Cell Biol.*, **22**, 5100–5113.
42. Liang, J., Kim, K.E., Schoderbek, W.E. and Maurer, R.A. (1992) Characterization of a non-tissue-specific, 3′,5′-cyclic adenosine monophosphate-responsive element in the proximal region of the rat prolactin gene. *Mol. Endocrinol.*, **6**, 885–892.
43. Shepard, A.R., Zhang, W. and Eberhardt, N.L. (1994) Two CGTCA motifs and a GHF1/Pit1 binding site mediate cAMP-dependent protein kinase A regulation of human growth hormone gene expression in rat anterior pituitary GC cells. *J. Biol. Chem.*, **269**, 1804–1814.
44. Struthers, R.S., Vale, W.W., Arias, C., Sawchenko, P.E. and Montminy, M.R. (1991) Somatotroph hypoplasia and dwarfism in transgenic mice expressing a non-phosphorylatable CREB mutant. *Nature*, **350**, 622–624.
45. Burton, F.H., Hasel, K.W., Bloom, F.E. and Sutcliffe, J.G. (1991) Pituitary hyperplasia and gigantism in mice caused by a cholera toxin transgene. *Nature*, **350**, 74–77.
46. Stevens, C.A., Hennekam, R.C. and Blackburn, B.L. (1990) Growth in the Rubinstein-Taybi syndrome. *Am. J. Med. Genet. Suppl.*, **6**, 51–55.
47. Oike, Y., Hata, A., Mamiya, T., Kaname, T., Noda, Y., Suzuki, M., Yasue, H., Nabeshima, T., Araki, K. and Yamamura, K. (1999) Truncated CBP protein leads to classical Rubinstein-Taybi syndrome phenotypes in mice: implications for a dominant-negative mechanism. *Hum. Mol. Genet.*, **8**, 387–396.
48. Bartholdi, D., Roelfsema, J.H., Papadia, F., Breuning, M.H., Niedrist, D., Hennekam, R.C., Schinzel, A. and Peters, D.J. (2007) Genetic heterogeneity in Rubinstein-Taybi syndrome: delineation of the phenotype of the first patients carrying mutations in EP300. *J. Med. Genet.*, **44**, 327–333.
49. Yang, Z., Huang, W., Lee, D., Copolov, D.L. and Lim, A.T. (1993) The adenylyl cyclase-cyclic AMP system modulates morphological and functional development of hypothalamic beta-endorphin neurons in culture. *J. Neuroendocrinol.*, **5**, 371–380.
50. Lee, D., Huang, W., Yang, Z., Copolov, D.L. and Lim, A.T. (1992) *In vitro* evidence for modulation of morphological and functional development of hypothalamic immunoreactive atrial natriuretic peptide neurons by cyclic 3′,5′-adenosine monophosphate. *Endocrinology*, **131**, 911–918.
51. Arumugam, H., Liu, X., Colombo, P.J., Corriveau, R.A. and Belousov, A.B. (2005) NMDA receptors regulate developmental gap junction uncoupling via CREB signaling. *Nat. Neurosci.*, **8**, 1720–1726.
52. Zhu, Y., Ghosh, P., Charnay, P., Burns, D.K. and Parada, L.F. (2002) Neurofibromas in NF1: Schwann cell origin and role of tumor environment. *Science*, **296**, 920–922.
53. Bajenaru, M.L., Hernandez, M.R., Perry, A., Zhu, Y., Parada, L.F., Garbow, J.R. and Gutmann, D.H. (2003) Optic nerve glioma in mice requires astrocyte Nf1 gene inactivation and Nf1 brain heterozygosity. *Cancer Res.*, **63**, 8573–8577.
54. Birnbaum, R.A., O'Marcaigh, A., Wardak, Z., Zhang, Y.Y., Dranoff, G., Jacks, T., Clapp, D.W. and Shannon, K.M. (2000) Nf1 and Gmcsf interact in myeloid leukemogenesis. *Mol. Cell*, **5**, 189–195.
55. Vogel, K.S., Klesse, L.J., Velasco-Miguel, S., Meyers, K., Rushing, E.J. and Parada, L.F. (1999) Mouse tumor model for neurofibromatosis type 1. *Science*, **286**, 2176–2179.
56. Cichowski, K., Shih, T.S., Schmitt, E., Santiago, S., Reilly, K., McLaughlin, M.E., Bronson, R.T. and Jacks, T. (1999) Mouse models of tumor development in neurofibromatosis type 1. *Science*, **286**, 2172–2176.
57. Xu, J., Ismat, F.A., Wang, T., Yang, J. and Epstein, J.A. (2007) NF1 regulates a Ras-dependent vascular smooth muscle proliferative injury response. *Circulation*, **116**, 2148–2156.
58. Schindeler, A., Morse, A., Harry, L., Godfrey, C., Mikulec, K., McDonald, M., Gasser, J.A. and Little, D.G. (2008) Models of tibial fracture healing in normal and Nf1-deficient mice. *J. Orthop. Res*. Epub March 26.
59. Szudek, J., Evans, D.G. and Friedman, J.M. (2003) Patterns of associations of clinical features in neurofibromatosis 1 (NF1). *Hum. Genet.*, **112**, 289–297.
60. Said, S.M., Yeh, T.L., Greenwood, R.S., Whitt, J.K., Tupler, L.A. and Krishnan, K.R. (1996) MRI morphometric analysis and neuropsychological function in patients with neurofibromatosis. *Neuroreport*, **7**, 1941–1944.
61. Margariti, P.N., Blekas, K., Katzioti, F.G., Zikou, A.K., Tzoufi, M. and Argyropoulou, M.I. (2007) Magnetization transfer ratio and volumetric analysis of the brain in macrocephalic patients with neurofibromatosis type 1. *Eur. Radiol.*, **17**, 433–438.
62. Cutting, L.E., Cooper, K.L., Koth, C.W., Mostofsky, S.H., Kates, W.R., Denckla, M.B. and Kaufmann, W.E. (2002) Megalencephaly in NF1: predominantly white matter contribution and mitigation by ADHD. *Neurology*, **59**, 1388–1394.